Control of DFIG-WT under unbalanced grid voltage conditions

Alvaro Luna*, *Student Member IEEE*, Kleber Lima**, Felipe Corcoles*, Edson Watanabe**, *Senior Member IEEE,* Pedro Rodriguez*, *Member IEEE*, Remus Teodorescu**, *Senior Member IEEE*.

*Technical University of Catalonia
C/ Colom 1 08222, Terrassa, Spain
luna@ee.upc.edu, corcoles@ee.upc.edu, prodriguez@ee.upc.edu

**Federal University of Rio de Janeiro
Caixa Postal 68504 Rio de Janeiro, Brazil
fkalima@gmail.com, watanable@coe.ufrj.br

***Aalborg University
Pontoppidanstraede 101, 9220 Aalborg, Denmark
ret@iet.aau.dk

***Abstract* -- The voltage oriented control in the synchronous reference frame (VOC-SRF) have been extensively used for controlling wind turbines based on doubly fed induction generators (DFIG-WTs) through the rotor side converter of a back to back power processor. Although its performance is fast and accurate under balanced conditions its behaviour is not good enough when the voltage of the mains is unbalanced, unless an independent control for the positive and the negative sequence is implemented. This paper proposes a new control system able to control the DFIG-WT under unbalanced conditions using a simple algorithm, which does not need to be implemented for both symmetrical components but on the static $\alpha\beta$ reference frame. The reliability of the presented system will be tested by means of PSCAD simulations under balanced and unbalanced grid conditions.**

***Index Terms*-- AC generators, Current Control, Electrical Engineering, Wind Power Generation.**

I. INTRODUCTION

The massive installation of wind power farms in the last years has been launched by the arrival of variable speed wind turbines (WT), which are able to produce electrical power for a wide range of wind conditions. Within this kind of generators those based on DFIGs, which are connected to the grid through back to back converters, constitute, at the present time, the 50% of the installed wind power worldwide [1]. The major advantage of these facilities lies in the fact that the power rate of the inverters is around the 25-30% of the nominal generator power [2]-[3].

Nowadays, fulfilling the new FRT requirements is an important challenge for wind power industry. In modern WTs the symbiosis between electrical machines and power electronics is permitting to achieve noticeable headways regarding that topic. The modern grid codes require not only avoiding the disconnection of WT during the fault, but injecting certain quantities of active and reactive power according to the patterns available in the standards.

Unsymmetrical faults constitute the 95% of voltage dips that affect the stator windings of the DFIG. Although DFIG-WTs are able to withstand this kind of sags without tripping, such faults give rise to torque ripple in the rotor, due to the appearance of negative sequence voltage components at the point of common coupling (PCC).

The classical control systems for DFIG-WTs based on voltage oriented control (VOC) theories, have been broadly used for controlling such systems under generic conditions [4]. However, this kind of controllers must be splitted for controlling the positive and negative sequence of the rotor currents, in order to control the torque ripple of the DFIG, and hence the active power oscillations [5]. Nevertheless, the resulting control loop is not as simple as the classical one, something that is a drawback considering that the main advantage of VOC was its simplicity.

The aim of this paper is to present a new control system for DFIG-WTs, called voltage oriented control in the rotor reference frame (VOC-RRF), able to control the generator when the voltage at the stator is unbalanced without introducing torque ripple.

II. THE DFIG-WT UNDER UNBALANCED CONDITIONS

The DFIG-WTs are very sensitive to grid voltage sags, as the stator of the generator is directly connected to the mains. Although there are different kind of sags [6], they all give rise to common problems in such machines [7]-[9] as: electromagnetic torque peaks and ripple, active/reactive power oscillations and inrush stator currents. The simulation results that appear in Fig.1 and Fig.2 show the response of the DCIG-WT when an A type and a C type voltage sag [10] affects its stator windings.

A. Electromagnetic torque

Fig.1(a) describes the electromagnetic torque behaviour of the DFIG when both faults occur. This variable experiences an important reduction during the fault period in all cases. This torque drop is even more critical for the symmetrical fault than for the non-symmetrical one, nevertheless, the non-symmetrical voltages of the C sag produce an important torque ripple, due to the circulation of a negative sequence magnetic flux in the air gap produced by the negative sequence voltage.

B. *Active and Reactive Power Behavior*

In Fig.1(b) the positive sequence voltages at the generator's terminals are plotted. In this figure it stands out how the overall voltage reduction is higher when an A sag appears, due to the fact that all phases are short-circuited to ground. On the other hand the increase of the negative sequence voltage when there is an unbalanced sag constitute a serious drawback, due to the appearance of torque ripple in the rotor's shaft.

The performance of the active power delivered to the grid by the DFIG is detailed in Fig.2(a). This graph show how the injected power during the fault period is reduced with respect the nominal magnitude in both sags. The lowest average value, during and after the fault, is reached when the A sag is applied. In turn, the electromagnetic torque ripple that appeared in Fig.1(a) for the C sag is translated into active power ripple as well.

In Fig.2(b) the post-fault reactive power peaks in both simulations is the most relevant characteristic. These overshoots are due to the flow of high reactive currents, which are demanded by the DFIG in order to recover the magnetic flux at the generator. These currents yields important voltage drops at the DFIG terminals when the sags are cleared.

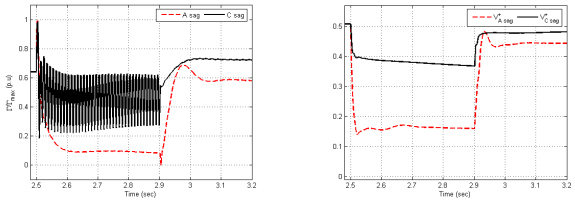

(a) (b)

Fig 1.- Response of a DFIG in front of two different voltage dips, A (dashed line) sag and C sag (continuous line).(a)-Electromagnetic torque of the DFIG ; (b)- Positive sequence voltage at the DFIG. In both cases the fault appears at t=2.5s and is cleared at t=2.9s

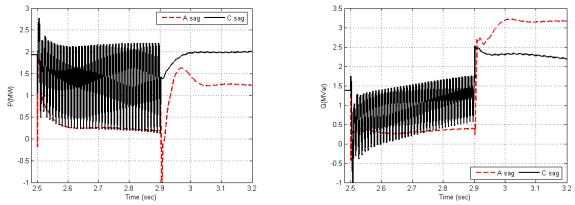

(a) (b)

Fig. 2.- Power and negative sequence voltage performance of a DFIG in front of two different voltage dips, A (dashed line) sag and C sag (continuous line).(a)-Active power delivered by the DFIG -WT during the fault and post fault periods ; (b)-Reactive power delivered by the DFIG -WT during the fault and post fault periods. In both cases the fault appears at t=2.5s and is cleared at t=2.9s

By means of this test it can be concluded that, despite the fact that the severity of the balanced fault can give rise to serious problems in the operation of DFIG-WTs, the appearance of negative sequence currents when unbalanced sags appear are very dangerous from the mechanical point of view.

III. Proposed Control Algorithm For the Rotor Side Converter

The control of the active/reactive power delivery through the stator of a DFIG-WT can be carried out considering a different point of view. In VOC-SRF techniques the rotor current setpoint is calculated by means of an external control loop, based on PI controllers, responsible of controlling the injection of *P* and *Q*. Therefore the dynamics of the control action lies on the performance of such controllers.

In applications where grid connected power converters are responsible of tracking a certain PQ reference, as shown in Fig.3, the necessary currents to be injected can be easily obtained using the instantaneous power theory.

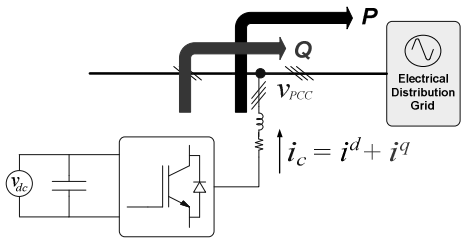

Fig. 3.- P and Q injection by means of a grid connected power converter

The instantaneous active and reactive powers related to generic voltage and current vectors, **v** and **i**, in a three-phase system can be written as detailed in (1)-(2).

$$p = \mathbf{v} \cdot \mathbf{i} \tag{1}$$

$$q = \left| \mathbf{v} \times \mathbf{i}^q \right| = \mathbf{v}_\perp \cdot \mathbf{i}^q \tag{2}$$

Where $\mathbf{v}_\perp$ are a set of in-quadrature signals with respect the measured grid voltage, $\mathbf{v}$, at the coupling point [17]. Both vectors are shown in the *abc* reference frame in Fig. 4.

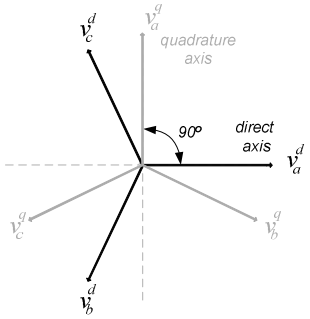

Fig. 4.- Components of the measured and in-quadrature voltages

Regarding (1) and (2) the currents that are needed to achieve a certain value of *P* at the stator windings can be calculated as:

$$\left[\vec{i}_{abc}^{\,d}\right] = \frac{P^*}{\left|\vec{v}_{abc}^{\,d}\right|^2} \cdot \vec{v}_{abc}^{\,d} \tag{3}$$

In (3) the measured stator voltage are represented by $\vec{v}_{abc}^{\,d}$, while the resulting stator currents are $\vec{i}_{abc}^{\,d}$. As it can be concluded from this equation, the unitary vector of the voltage, that defines the frequency and phase of the currents, is aligning $\vec{i}_{abc}^{\,d}$ with the stator voltage and, as a consequence, any current injected in this direction will produce only active power.

Likewise, the injection of reactive power could be achieved by injecting currents in-quadrature with the stator voltage (4).

$$\left[\vec{i}_{abc}^{\,q}\right] = \frac{Q^*}{\left|\vec{v}_{abc}^{\,q}\right|^2} \cdot \vec{v}_{abc}^{\,q} \tag{4}$$

In (4) $\vec{v}_{abc}^{\,q}$ is a three-phase signal with the same amplitude and frequency of the stator voltage, but shifted 90º, as shown in Fig.vec. The addition of $\vec{i}_{abc}^{\,d}$ and $\vec{i}_{abc}^{\,q}$ give rise finally to the currents to be delivered by the converter in order to provide the desired P^* and Q^* simultaneously, as written in (5).

$$\vec{i}_{abc} = \vec{i}_{abc}^{\,d} + \vec{i}_{abc}^{\,q} \tag{5}$$

A similar reasoning can be conducted for determining the necessary rotor currents to be injected by the RSC of a DFIG in order to deliver a certain *P* and *Q*. As displayed in Fig. 5, in this generation facilities the DFIG acts as an interface between the RSC and the network.

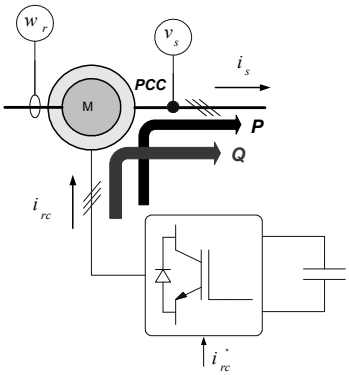

Fig. 5.- Control of P and Q injection by means of the RSC of a DFIG

However, the direct, *d*, and quadrature, *q*, current components at the stator windings can be controlled through the rotor, and hence it is possible to determine the shape of the currents to be injected at the rotor side in order to obtain the desired output power at the stator.

A. Stator Power Control in the Rotor Reference Frame

For controlling the *P* and *Q* through the rotor it is necessary to transform the stator variables into the Rotor Reference Frame (RRF). The DFIG can be understood as a rotational transformer, therefore it is possible to predict which current delivered through the rotor will produce a determined stator current just knowing the phase between the rotor and stator windings. This phase has been depicted in Fig.6.

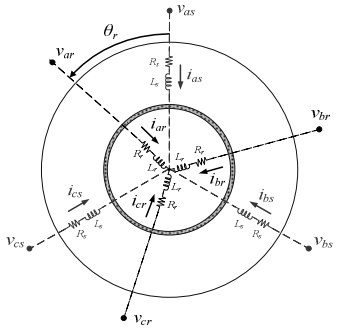

Fig. 6.- Distribution of the stator/rotor windings in a DFIG

The direct stator voltage components in the rotor reference frame can be found thanks to (6):

$$\left[\vec{v}_{\alpha\beta_{rs}}^{\,d}\right] = [\Gamma][\mathrm{M}][\vec{v}_{abc}] \tag{6}$$

In (6) M is the classical Clarke transformation, and, Γ is the rotation matrix that can be written as:

$$[\Gamma] = \begin{bmatrix} \cos\theta_r & \sin\theta_r \\ -\sin\theta_r & \cos\theta_r \end{bmatrix} \tag{7}$$

where θ_r is the electrical angle of the rotor, that is equal to the mechanical angle multiplied by the pair of poles of the generator. Likewise the in-quadrature voltage vector can be found as shown in (8).

$$\left[\vec{v}_{\alpha\beta_{rs}}^{\,q}\right] = [\mathrm{H}][\Gamma][\mathrm{M}][\vec{v}_{abc}] \tag{8}$$

In this second case the H matrix, as detailed in (9), permits obtaining the in-quadrature voltages in the $\alpha\beta$ reference frame.

$$\left[\vec{v}_{\alpha\beta}^{\,q}\right] = [\mathrm{H}]\left[\vec{v}_{\alpha\beta}^{\,d}\right] \;;[\mathrm{H}] = \begin{bmatrix} 0 & -1 \\ 1 & 0 \end{bmatrix} \tag{9}$$

According to (3) and (4) the voltage vectors, $\vec{v}_{\alpha\beta_{rs}}^{\,d}$ and $\vec{v}_{\alpha\beta}^{\,q}$, permits calculating the instantaneous value of the currents. Therefore the rotor currents that are necessary for injecting a certain *P** and *Q** through the stator can be found, in the DFIG case as:

$$\left[\vec{i}^{\,*}_{\alpha\beta_r}\right]=\frac{P^*}{\left|\vec{v}^{\,d}_{\alpha\beta_{rs}}\right|^2}\left[\vec{v}^{\,d}_{\alpha\beta_{rs}}\right]+\frac{Q^*}{\left|\vec{v}^{\,d}_{\alpha\beta_{rs}}\right|^2}\left[\vec{v}^{\,q}_{\alpha\beta_{rs}}\right] \quad (10)$$

where $\left|\vec{v}^{\,d}_{\alpha\beta_{rs}}\right|$ is the magnitude of the vector, shown in (11):

$$\left|\vec{v}^{\,d}_{\alpha\beta_{rs}}\right|=\sqrt{\left(v^d_{\alpha_{rs}}\right)^2+\left(v^d_{\beta_{rs}}\right)^2} \quad (11)$$

and $\left[\vec{v}^{\,d}_{\alpha\beta_{rs}}\right]$ and $\left[\vec{v}^{\,q}_{\alpha\beta_{rs}}\right]$ are the already deducted direct and in-quadrature voltages of the stator in the rotor reference frame.

The value of the rotor currents to be injected is then the result of the addition between the active and reactive components, as it stands out clearly in (12), where (10) has been extended.

$$\begin{bmatrix} i^*_{\alpha_r} \\ i^*_{\beta_r} \end{bmatrix}=\underbrace{\frac{P^*}{\left|\vec{v}^{\,d}_{\alpha\beta_{rs}}\right|^2}\cdot\begin{bmatrix} v^d_{\alpha_{rs}} \\ v^d_{\beta_{rs}} \end{bmatrix}}_{Active}+\underbrace{\frac{Q^*}{\left|\vec{v}^{\,d}_{\alpha\beta_{rs}}\right|^2}\cdot\begin{bmatrix} v^q_{\alpha_{rs}} \\ v^q_{\beta_{rs}} \end{bmatrix}}_{Reactive} \quad (12)$$

The P^* and Q^* values correspond to the desired output at the stator windings. However the electrical generator itself takes a certain value of Q and P, due to their magnetic fields and internal losses, which are not being considered, as far as they are unknown most of the times.

Therefore, it is also necessary to include an auxiliary PI controller, able to correct this error. This structure is shown in Fig.7. As it can be concluded from the figure, the error in P increase the direct component of the rotor current, while the error in Q affects the in-quadrature components.

The layout of the proposed control topology for the rotor side converter of the DFIG is shown graphically in Fig. 8.

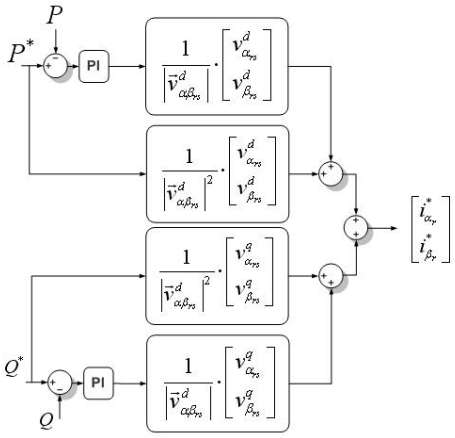

Fig 7 .- Auxliar PI controller for controlling P and Q errors

As it is depicted in the figure the stator voltage, as well as the active and reactive power set points, constitute the main references in this control structure. Those signals are later processed by the different blocks of the VOC-RRF algorithm, determining finally a rotor current set point for the rotor side converter.

B. *Current control loop*

As a difference with VOC-SRF controllers, the presented VOC-RRF proposal implements the current control in the $\alpha\beta$ domain, as shown in Fig.8, by means of frequency adaptive resonant controllers.

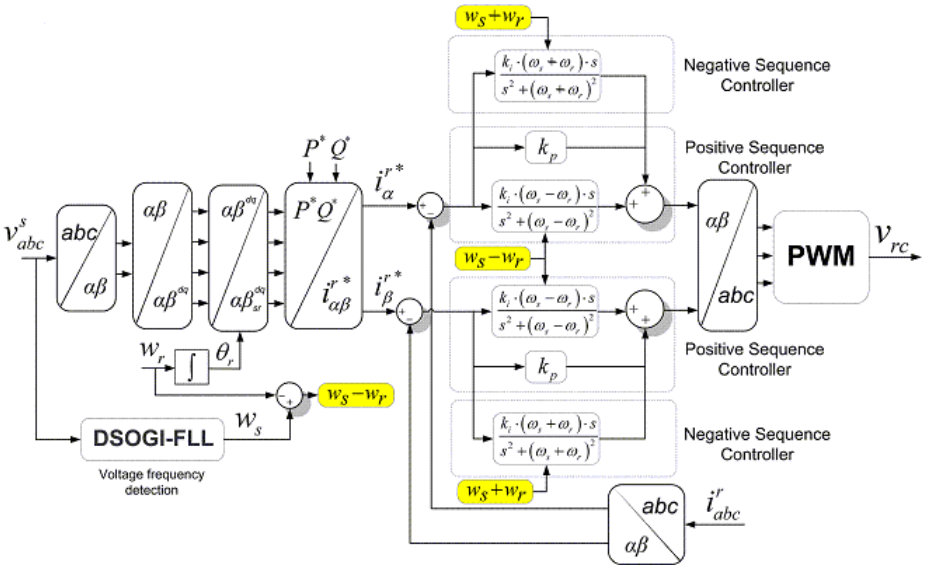

Fig 8.- VOC-RRF control of the rotor-side power converter in the $\alpha\beta$ reference frame.

As it is broadly discussed in [11] and [12], such controllers are able to perform exactly the same dynamical response than a classical PI in a synchronous reference frame. Nevertheless resonant controllers require only the tuning of the resonance frequency, while for a PI based control the phase estimation must be provided.

In grid connected generation facilities, the frequency of the grid rarely experience jumps, and its value normally remains among a narrow margin. On the contrary, the phase of the voltage is not as constant as the frequency, and under transient the phase at the stator windings of a DFIG can experience sudden jumps around 40º-60º, as shown in [13]-[14]. For this reason a control system based on a PLL, that detects the phase of the voltage, which is later used for setting the synchronous reference frame of the control system is less robust if compared with another system that only needs to detect the frequency of the network, thanks to a Frequency Locked Loop (FLL), as in the VOC-RRF case.

In this particular case the current set point for the proportional resonant (PR) controller has a variable frequency, equal to the slip of the generator. The transfer function of this controller is written in (13).

$$|PR| = k_p + \frac{k_i (w_s - w_r) s}{s^2 + (w_s - w_r)^2} \qquad (13)$$

The second term of (13) is a second order generalized integrator (SOGI) [15]-[17]. This kind of transfer function has been broadly used in grid-synchronization applications, and permits to cancel out the error in the current injection at the specified frequency.

The current controller can be extended to the negative sequence components just by adding another resonant controller tuned at $w_s + w_r$, that would permit to inject negative sequence currents. The implementation of this dual controller in the VOC-RRF is simpler than in the classical VOC-SRF where a new rotating reference frame must be set.

IV. Simulation Platform and Results

The performances of the VOC-SRF and VOC-RRF control systems presented in this paper have been tested in simulation using PSCAD/EMTDC. The layout of the model is depicted in Fig.9, where the DFIG parameters that are implemented in the simulation are shown in Table I.

In this model the power converters are controlled as current sources, using commutated models of IGBT converters that are driven by means of PWM signals, whose carrier frequency is equal to 10 kHz.

In a first simulation test the power tracking behaviour of the VOC-RRF and VOC-SRF, under voltage balanced grid conditions, has been analyzed by means of applying an active power step to the set point of both control systems.

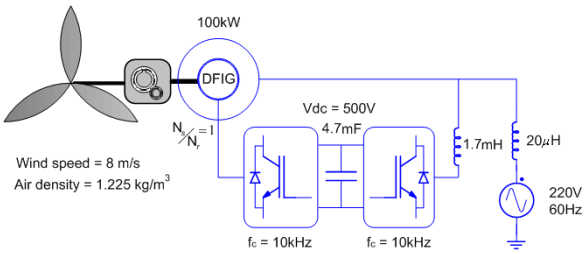

Fig 9.- Simulation model programmed in PSCAD

In Fig.10 the behaviour of the classical VOC-SRF is shown. In Fig.10.a the comparison between the active power setpoint and the real power delivered through the stator is displayed, in this particular case the DFIG reduce the power delivery from 90 kW to 75 kW. As a consequence the speed of the rotor increases, something that can be easily noticed in Fig.10.b where the speed in p.u is shown. In Fig.10.c the change in the stator currents are printed, while the rotor currents appear in Fig.10.d. In both cases the change in the active power setpoint is translated into a smooth variation of the amplitude in the current waveforms as well as in the frequency value.

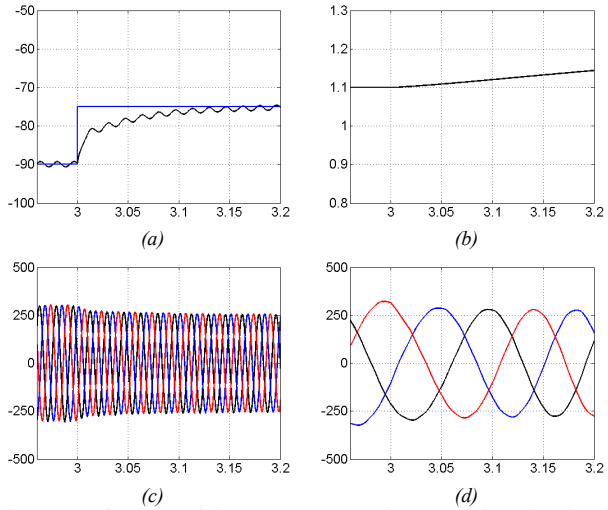

Fig 10.- Performance of the VOC-SRF control strategy when changing the active power setpoint. (a) Active power jump; (b) Speed of the DFIG; (c) Currents at the stator windings; (d) Currents injected by the rotor side converter.

The same test was performed using the VOC-RRF as the control algorithm for the rotor side converter.

In Fig.11.a it can be seen how the proposed system follows rapidly the active power setpoint. In this case the tunning of the parameters has made this controller a little bit faster than the previous one. This is the reason why the stator and rotor currents, available in Fig.11.c and Fig.11.d changed with a faster transient.

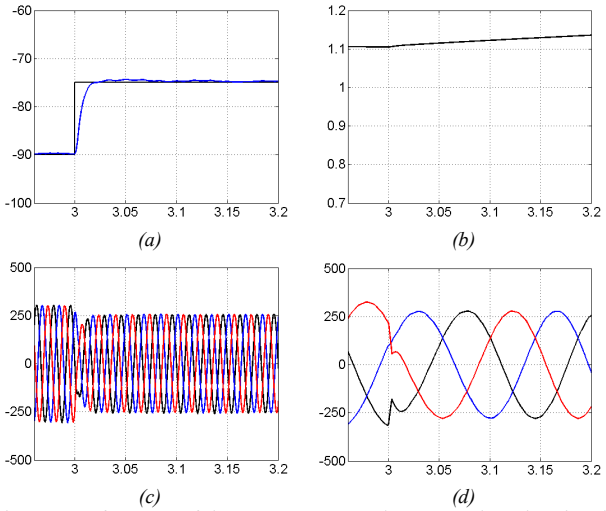

Fig 11.- Performance of the VOC-RRF control strategy when changing the active power setpoint. (a) Active power jump; (b) Speed of the DFIG; (c) Currents at the stator windings; (d) Currents injected by the rotor side converter.

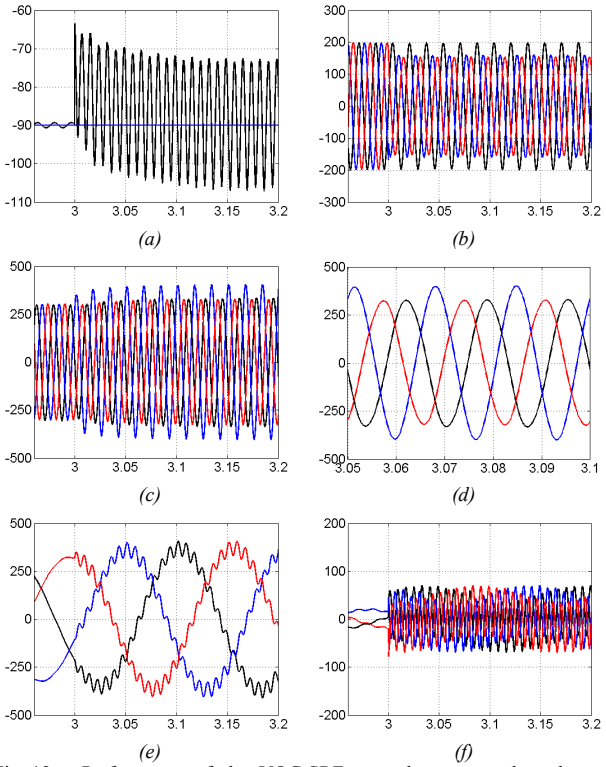

Fig 12.- Performance of the VOC-SRF control strategy when the grid voltage is unbalanced (a) Active power delivery; (b) Grid voltage waveforms; (c) Currents at the stator windings; (d) Zoom of the stator currents between 3.05 and 3.1 sec.; (e) Currents injected by the rotor side converter; (f) Voltage at the rotor windings (filtered).

More significant differences between both controllers can be found when the grid voltage becomes unbalanced. These conditions where reproduced in a second simulation test, where the grid voltage became unbalanced after t = 3s.

In Fig 12 the behaviour of the VOC-SRF under such conditions is shown. In Fig.12.b the grid voltage waveforms show how in t = 3s a negative sequence component appeared in the three phase signal. In Fig.12.a it can be realized how the active power delivered through the stator begins to oscillate.

The currents in the stator are shown in Fig.12.c and Fig.12.d, being the second one a zoom performed around 3 – 3.05 sec. The behavior of the rotor currents have been displayed in Fig.12.e. In this plot it can be noticed how the rotor converter is trying to inject some negative sequence voltage. However as a classical controller has been implemented the system is unable to control this sequence, giving rise to power oscillations in the stator. In addition the voltage unbalance affects negatively the estimation of the flux position that is necessary for the VOC-SRF control. Finally a filtered signal of the rotor voltage is depicted in Fig.12.f.

The same test was done using the proposed VOC-RRF. In this case, due to the fact that a current control for the negative sequence can be easily implemented just by adding a resonant controller, the results regarding the active power delivery were better. In Fig.13.a the active power delivered through the stator show a little ripple,that can be almost neglected when the unbalance voltage appear.

The stator currents that where calculated thanks to (3) give rise to current waveforms that produce a constant active power delivery. These currents are shown in Fig.13.c and Fig.13.d.

The shape of this stator currents are controlled through the rotor converter, that injects the appropriate currents in the rotor to synthesize the desired stator currents according to (12). As in the previous case the rotor side voltage is shown in Fig.13.e, in order to show that the voltage in these windings remain between controllable limits.

In this point it is important to highlight that none of the tested algorithms have produced overcurrents or overvoltages, yielding a stable operating conditions when transients in the active power or in the grid voltage occur.

In addition, the simulation results have proven that both control algorithms are able to offer satisfactory results under grid voltage balanced conditions. However remarkable differences can be found when the voltage is unbalanced.

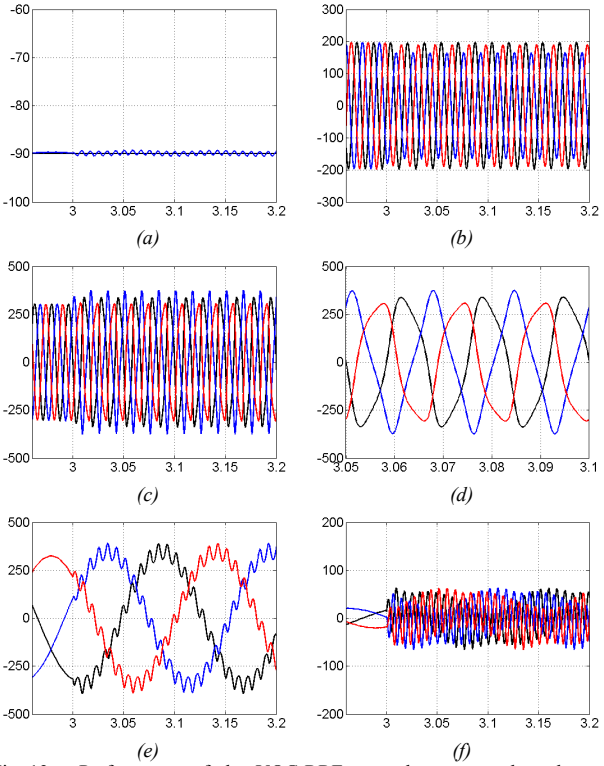

Fig 13.- Performance of the VOC-RRF control strategy when the grid voltage is unbalanced (a) Active power delivery; (b) Grid voltage waveforms; (c) Currents at the stator windings; (d) Zoom of the stator currents between 3.05 and 3.1 sec.; (e) Currents injected by the rotor side converter; (f) Voltage at the rotor windings (filtered).

V. CONCLUSIONS

The proposed control strategy permits to control a DFIG under unbalanced grid voltage conditions. As a difference with previous methods, based on VOC on the synchronous *dq* reference frame, this control is simpler, as it based on adaptive frequency resonant controllers. This kind of current control does not need to work in a synchronous reference frame, something that permits building control loops for the positive and the negative sequence easier.

Moreover the presented control introduce a fedforward concept to determine the rotor currents to be injected. Depending on the desired power delivery different current set points can be easily applied as the reference for the rotor side converter controller.

ACKNOWLEDGMENT

This work was supported by the projects ENE2008-06841-C02-01/ALT and ENE2008-06588-C04-03/ALT financed by the Ministerio de Ciencia e Innovacion of Spain.

APPENDIX

Tables I gathers the parameters of the doubly-fed induction generator used in the simulations of this paper.

TABLE I
SPECIFICATION OF THE SIMULATED SYSTEMS.

Machine parameters	Values
Rated power	100 kVA
Rated stator voltage	220 V
Rated rotor voltage	220 V
Rated estator current	340 A
Rated stator frequency	60 Hz
Stator resistance	2.6 mΩ
Rotor resistance	2.9 mΩ
Stator leakage inductance	138.66 µH
Rotor leakage inductance	141.22 µH
Mutual inductance	5.6 mH
Angular moment of inertia (J=2H)	0.5 pu
Poles pairs	1

REFERENCES

[1] Blaabjerg, F. ; Chen, Z., "Power Electronics for Modern Wind Turbines" *Synthesus Lectures on Power Electronics,* 2006

[2] Akhmatov, V.; "Analysis of dinamical behavior of electric power systems with large amount of wind power". *PhD dissertation Orsted-DTU,* 2003.

[3] R. W. De Doncker and D. W. Novotny, "The universal field oriented controller". IEEE Transactions on Industry Applications, vol. 30, No 1, p. 92-100, 1994.

[4] Pena, R.; Clare, J. & Asher, G. "A doubly fed induction generator using back-to-back PWM converters supplying an isolated load from a variable speed wind turbine". *Electric Power Applications, IEE Proceedings-,* 1996, *143*, 380-387

[5] Xu, L.; Wang, Y.; "Dynamic Modeling and Control of DFIG-Based Wind Turbines Under Unbalanced Network Conditions". *Power Systems, IEEE Transactions on,*2007, 20, 314 -323.

[6] M. Bollen, "Voltage sags in three-phase systems," *Power Engineering Review, IEEE*, vol. 21, no. 9, pp. 8–11,15, Sept. 2001.

[7] F. Corcoles and J. Pedra, "Algorithm for the study of voltage sags on induction machines," *Energy Conversion, IEEE Transactions on*, vol. 14, no. 4, pp. 959–968, Dec. 1999.

[8] L. Guasch, F. Corcoles, and J. Pedra, "Effects of symmetrical and unsymmetrical voltage sags on induction machines," *Power Delivery, IEEE Transactions on*, vol. 19, no. 2, pp. 774–782, April 2004

[9] L. Guasch, "Efecto de los huecos de tension en las maquina de induccion y en los transformadores trifasicos," Ph.D. dissertation, UPC, 2006.

[10] L. Zhang and M. Bollen, "Characteristic of voltage dips (sags) in power systems," *Power Delivery, IEEE Transactions on*, vol. 15, no. 2, pp. 827–832, 2000.

[11] P. Mattavelli, "A closed-loop selective harmonic compensation for active filters ," Industry Applications, IEEE Transactions on , vol.37, no.1, pp.81-89, Jan/Feb 2001

[12] D.N. Zmood, D.G. Holmes, "Stationary frame current regulation of PWM inverters with zero steady-state error," Power Electronics, IEEE Transactions on , vol.18, no.3, pp. 814-822, May 2003

[13] Bollen, M. "Characterisation of voltage sags experienced by three-phase adjustable-speed drives" *Power Delivery, IEEE Transactions on,* 1997, 12, 1666-1671

[14] Styvaktakis, E. & Bollen, M. "Signatures of voltage dips: transformer saturation and multistage dips" *Power Delivery, IEEE Transactions on,* 2003, 18, 265-270

[15] Blaabjerg, F.; Teodorescu, R.; Liserre, M. & Timbus, A.;"Overview of Control and Grid Synchronization for

Distributed Power Generation Systems" *Industrial Electronics, IEEE Transactions on,* 2006, 53, 1398-1409

[16] Rodriguez, P.; Luna, A.; Ciobotaru, M.; Teodorescu, R. & Blaabjerg, F. "Advanced Grid Synchronization System for Power Converters under Unbalanced and Distorted Operating Conditions"
Industrial Electronics, 2006 IEEE 32th Conference on, 2006.

[17] Yuan, X., Merk, W., Stemmler, H., and Allmeling, J., "Stationary frame generalized integrators for current control of active power filters with zero steady-state error for current harmonics of concern under unbalanced and distorted operating conditions," *IEEE Trans. Ind. Appl.*, vol. 38, no.2, pp. 523–532, Mar./Apr. 2002.